

Transitions and spin dynamics at very low temperature in
the pyrochlores $\text{Yb}_2\text{Ti}_2\text{O}_7$ and $\text{Gd}_2\text{Sn}_2\text{O}_7$

P. BONVILLE, J. A. HODGES, E. BERTIN, J.-PH. BOUCHAUD, M. OCIO,

C.E.A.- Saclay, Service de Physique de l'Etat Condensé
91191 Gif-sur-Yvette, France

AND

P. DALMAS DE RÉOTIER, L.-P. REGNAULT, H. M. RØNNOW, J. P.
SANCHEZ, S. SOSIN, A. YAOUANC

C.E.A.- Grenoble, Service de Physique Statistique, de Magnétisme et
Supraconductivité
38054 Grenoble, France

AND

M. RAMS, K. KRÓLAS

Institute of Physics, Jagellonian University, 30059 Kraków, Poland

The very low temperature properties of two pyrochlore compounds, $\text{Yb}_2\text{Ti}_2\text{O}_7$ and $\text{Gd}_2\text{Sn}_2\text{O}_7$, were investigated using an ensemble of microscopic and bulk techniques. In both compounds, a first order transition is evidenced, as well as spin dynamics persisting down to the 20 mK range. The transition however has a quite different character in the two materials: whereas that in $\text{Gd}_2\text{Sn}_2\text{O}_7$ (at 1 K) is a magnetic transition towards long range order, that in $\text{Yb}_2\text{Ti}_2\text{O}_7$ (at 0.24 K) is reminiscent of the liquid-gas transition, in the sense that it involves a 4 orders of magnitude drop of the spin fluctuation frequency; furthermore, no long range order is observed. These unusual features we attribute to frustration of the antiferromagnetic exchange interaction in the pyrochlore lattice.

PACS numbers: 75.40.-s, 75.25.+z, 76.75.+i, 76.80.+y

1. Introduction

Frustration of exchange interactions among magnetic ions can arise in different ways: the first to be studied was frustration induced by crystallo-

graphic disorder, leading to the so-called spin glass materials. Frustration can also appear in fully crystallographically ordered materials, if the geometry of the lattice is such that it prevents all pairs of exchange bonds from being satisfied throughout the lattice. The simplest example is the bidimensional triangular lattice with isotropic (Heisenberg) antiferromagnetic (AF) nearest neighbour exchange. Villain drew attention to geometrically frustrated systems [1] and showed that no Néel order can occur in a Heisenberg antiferromagnet on a three-dimensional lattice of corner sharing tetrahedra. The ground state of such a system was called a “cooperative paramagnet”, or a “spin liquid” state, where the spins undergo short range dynamic correlations down to $T = 0$. In the past decade, investigations of geometrically frustrated systems have developed to a large extent [2], and a number of lattices have been shown to be prone to frustration: the bidimensional *kagomé* lattice, made of corner-sharing coplanar triangles, the pyrochlore lattice, made of corner-sharing tetrahedra, and the garnet lattice, made of non-coplanar corner sharing triangles.

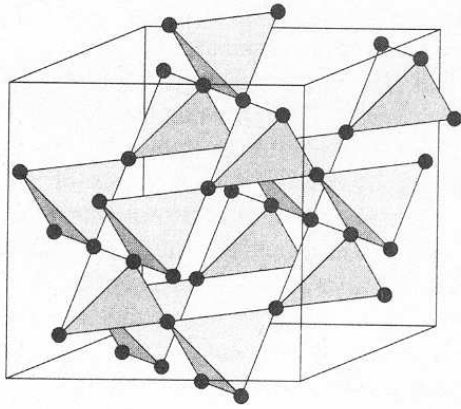


Fig. 1. The pyrochlore lattice of $R_2M_2O_7$ materials, where only the R sublattice is shown (black dots); for each R^{3+} ion, the local symmetry is threefold, with the appropriate local $[111]$ axis as symmetry axis.

The formation of the ground state and the low temperature spin dynamics have been particularly studied for the case of the Heisenberg antiferromagnet in a pyrochlore lattice with nearest neighbour exchange [3]. The ground state configuration is shown to have a large degeneracy, stemming from the energy minimizing condition: $\sum_i \mathbf{S}_i = 0$, where the sum runs over the spins \mathbf{S}_i of a “plaquette” or a “unit”, i.e. either a triangle or a tetrahedron. These ground states are not separated by energy barriers, and this

can have important implications as regards the spin dynamics: zero energy local or extended soft modes are possible, even at very low temperature. Another consequence is that any perturbation, like the dipole-dipole interaction, next nearest neighbour exchange, ionic or exchange anisotropy, can select a particular ground state, resulting in a transition at a finite temperature. The perturbations can also alter the flat energy landscape and create energy barriers between ground configurations, which suggests that real frustrated pyrochlore systems can retain some features of spin-glasses.

Compounds with formula $R_2M_2O_7$, where R is a rare earth and M a transition or *sp* metal, crystallise in a structure where both R and M ions are located at the vertices of two interpenetrating corner sharing tetrahedra, or pyrochlore, lattices (Fig.1). In the course of our study of rare earth pyrochlores, we have discovered novel behaviours in two materials, $Yb_2Ti_2O_7$ and $Gd_2Sn_2O_7$, which are the subject of this report. In these compounds, the rare earth alone is magnetic and it is located at a site with threefold symmetry (D_{3d}). The paramagnetic Yb^{3+} ($4f^{13}$) and Gd^{3+} ($4f^7$) ions have distinct single ion properties: the crystal electric field splits the ground spin-orbit multiplet $\{J = 7/2\}$ of the Yb^{3+} ion into 4 Kramers doublets, whereas it has practically no influence on the Gd^{3+} ion which has $L = 0$ and $S = 7/2$. This implies that the ground Yb^{3+} Kramers doublet, which alone is populated at low temperature, is described by an effective spin 1/2 with a g-tensor having uniaxial anisotropy, whereas the Gd^{3+} ion is isotropic and has a g-factor very close to 2.

Our investigations were carried out using local techniques: Mössbauer spectroscopy on the isotopes ^{170}Yb and ^{155}Gd , Muon Spin Relaxation (μ SR) spectroscopy, Perturbed Angular Correlations (PAC) on the isotope ^{172}Yb and neutron diffraction on the one hand, and bulk measurements: magnetic susceptibility and specific heat on the other hand. Most of these measurements were performed down to the 20 mK temperature range.

2. $Yb_2Ti_2O_7$

In $Yb_2Ti_2O_7$, a sharp peak in the specific heat had been evidenced near 0.24 K [4] (Fig.2 left), but the nature of the transition had not been further investigated. A broad feature, peaking around 2-3 K, is also visible. As will be shown below, the ground crystal field doublet of the Yb^{3+} ion is well isolated from the excited states. Therefore, the broad feature cannot be assigned to a crystal field Schottky anomaly, but it must be attributed to exchange spin correlations. The entropy released at the transition amounts to only 20% of the total magnetic entropy associated with a doublet, $R \ln 2$. This behaviour shows that the correlations develop far above the temperature of the transition (0.24 K), which is a characteristic feature of frustrated

systems [2].

In order to assess the crystal field splitting in this material, we performed PAC experiments on the isotope ^{172}Yb , which allow the thermal variation of the electric field gradient (EFG) tensor at the nucleus site to be measured. In axial symmetry, the EFG tensor is specified by its principal component $V_{zz} = \frac{\partial^2 V}{\partial z^2}(\mathbf{r} = 0)$ alone, which is the sum of two terms:

$$V_{zz}(T) = V_{zz}^{latt} + B_Q \langle 3J_z^2 - J(J+1) \rangle_T. \quad (1)$$

The first term is a temperature independent lattice charge contribution, and the second term is proportional to the $4f$ shell quadrupole moment, which is temperature dependent due to the progressive population of the crystal field levels as temperature increases.

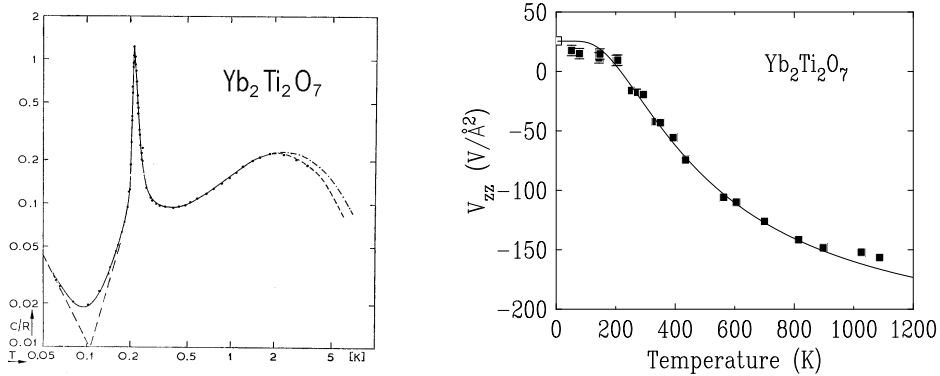


Fig. 2. In $\text{Yb}_2\text{Ti}_2\text{O}_7$: **Left**: Specific heat (from Ref.[4]), and **Right**: thermal variation of the principal component V_{zz} of the electric field gradient at the nucleus site as measured by PAC on ^{172}Yb (solid symbols) and ^{170}Yb Mössbauer spectroscopy (open symbol); the line is a fit to a crystal electric field model (see text).

The quantity $V_{zz}(T)$ decreases monotonously as temperature increases (Fig.2 right), and tends to V_{zz}^{latt} at high temperature ($\simeq -200 \text{ V}/\text{\AA}^2$) because the $4f$ shell term vanishes when all the crystal field states are equipopulated. One observes that $V_{zz}(0)$ is quite small, which is to a coincidental cancellation of the lattice and saturated $4f$ contributions, which are of opposite signs and of comparable magnitudes. We also performed Mössbauer experiments at 4.2 K on ^{170}Yb diluted in non-magnetic $\text{Y}_2\text{Ti}_2\text{O}_7$, which enabled us to measure the axially symmetric hyperfine tensor associated with the ground crystal field doublet. This tensor is proportional to the spectroscopic g-tensor, which is found to have components: $g_z \simeq 1.80$ and $g_{\perp} \simeq 4.27$. This shows that the plane perpendicular to the local $[111]$ axis is an easy magnetic plane for the Yb^{3+} ion at low temperature. From both the

$V_{zz}(T)$ thermal variation and the measurement of the ground state g-tensor (assuming that the latter is identical for Yb in $Y_2Ti_2O_7$ and in $Yb_2Ti_2O_7$), we could determine the full Yb^{3+} crystal field level scheme [5] in $Yb_2Ti_2O_7$. In particular, the 3 excited doublets lie at 620, 740 and 940 K above the ground state. At low temperature, the physics is therefore governed by the anisotropic ground Kramers doublet alone.

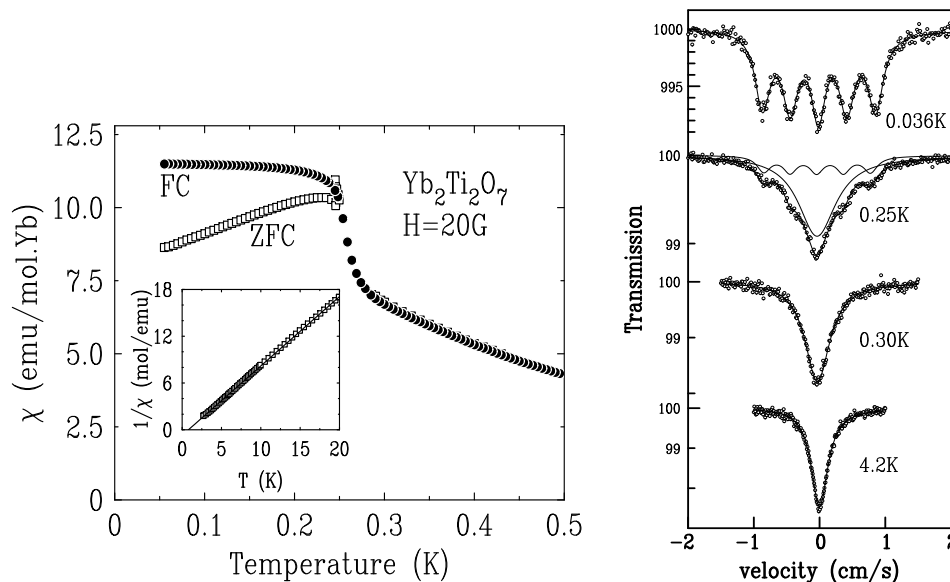


Fig. 3. In $Yb_2Ti_2O_7$: **Left**: magnetic susceptibility below 0.5 K showing the two FC and ZFC branches (inset: inverse susceptibility up to 20 K), and **Right**: selected ^{170}Yb Mössbauer absorption spectra between 0.036 K and 4.2 K; the lines are fits as explained in the text.

The magnetic susceptibility $\chi(T)$ follows a Curie-Weiss law below about 50 K, with a small positive paramagnetic Curie temperature $\theta_p \simeq 0.8$ K (inset of Fig.3 left). This can be indicative of a ferromagnetic net exchange interaction of magnitude *ca.* 1 K, but it does not preclude the presence of larger nearest and next nearest neighbour couplings with opposite signs. This latter assumption seems to be supported by the neutron diffraction data on a single crystal, to be described below. At 0.24 K, the temperature of the specific heat peak, an anomaly is seen in $\chi(T)$ (Fig.3 left). Below 0.24 K irreversibilities between the Field Cooled (FC) and Zero Field Cooled (ZFC) branches appear, which are reminiscent of a spin-glass behaviour.

Selected Mössbauer absorption spectra on the isotope ^{170}Yb ($I_g=0$, $I_e=2$, $E_0 = 84.3$ keV), represented in Fig.3 right, reveal an apparently standard first order magnetic transition at 0.24 K. At 0.036 K, a five-line

magnetic hyperfine pattern is observed with a hyperfine field $H_{hf} \simeq 115$ T corresponding to a saturated Yb^{3+} moment of *ca.* $1.15 \mu_B$. As temperature increases, the spectrum remains unchanged up to 0.22 K; then a broad single line grows superimposed on the five-line spectrum, and at 0.26 K the single line alone is left. In the temperature range $0.036 \text{ K} \leq T \leq 0.26 \text{ K}$, the hyperfine field associated with the five-line spectrum remains essentially constant. This fact and the coexistence, in a small temperature region, of the five-line pattern and of the single line, is characteristic of a first order transition. In principle, for a first order transition, one phase transforms into the other at the transition temperature by absorbing or releasing latent heat. In real systems, however, there is a narrow distribution of transition temperatures among the crystallites; this leads to the coexistence of the two phases in a small region around the mean transition temperature.

For an anisotropic Kramers doublet, the saturated moment value depends on the orientation of the applied or exchange field and, except when the field is along a principal direction of the g -tensor, the moment and the field are not collinear. The relationship linking the modulus m of the saturated moment and the angle θ it makes with the local z -axis is [5]:

$$\cos^2 \theta = \frac{\left(\frac{m_{\perp}}{m}\right)^2 - 1}{r^2 - 1}, \quad (2)$$

where $m_{\perp} = \frac{1}{2}g_{\perp}\mu_B$ and $r = g_{\perp}/g_z$. In $\text{Yb}_2\text{Ti}_2\text{O}_7$ below 0.24 K, from the measured m value and known r value, the angle between the moment and the local [111] axis is: $\theta \simeq 45^\circ$. So the Yb moment does not lie in the easy plane perpendicular to [111]; the angle φ the exchange field makes with the local z -axis can also be obtained through the relation: $\tan \theta = r^2 \tan \varphi$. One gets: $\varphi \simeq 10^\circ$. So the exchange field is almost directed along the threefold symmetry axis. At the present time, the origin of these angles cannot be reasonably interpreted, but they may provide clues for a future investigation of the spin configuration in $\text{Yb}_2\text{Ti}_2\text{O}_7$.

The characteristic time scale in these experiments is the hyperfine Larmor period for ^{170}Yb , which is about 10^{-9} s. This value is in fact the center of the ^{170}Yb ‘‘Mössbauer window’’ where the spin fluctuation frequency can be measured from the lineshape [6]. This has two consequences in the present case. First, it cannot be said whether the hyperfine field spectra observed below 0.24 K correspond to a static long range order (LRO) or to dynamic short range correlations with fluctuation frequencies smaller than the lower limit $\nu_l \simeq 10^8 \text{ s}^{-1}$ of the ‘‘Mössbauer window’’. This problem will be dealt with below when describing the neutron diffraction and μSR experiments. Second, the spectra above 0.24 K show a single line whose width decreases as temperature increases: this is the fingerprint of the ‘‘extreme narrowing’’ regime, where the spin fluctuation frequency is much larger than

the hyperfine coupling and increases as temperature increases. The fluctuation frequency can be measured as long as it is below the upper limit of the “Mössbauer window” for ^{170}Yb , i.e. $\nu_u \sim 5 \times 10^{10} \text{ s}^{-1}$. A physical hypothesis about the fluctuations is also needed: for paramagnetic fluctuations, a lineshape of the type developed in Ref.[6] is adequate, but for hyperfine field fluctuations (I.e. correlated moments), a stochastic lineshape as described in Ref.[7] must be used. In $\text{Yb}_2\text{Ti}_2\text{O}_7$, the neutron diffraction measurements on a single crystal, to be described below, show that spin correlations are present well above 0.25 K. So we interpret the spectra in the temperature range $0.25 \text{ K} \leq T \leq 0.9 \text{ K}$ in terms of hyperfine field fluctuations, where \mathbf{H}_{hf} jumps isotropically at random with a characteristic frequency ν [7]. Then the dynamical broadening of the Mössbauer spectrum in the “extreme narrowing” regime is given by:

$$\Delta\Gamma_R = \frac{\nu_{hf}^2}{\nu}, \quad (3)$$

where the hyperfine frequency ν_{hf} is $\mu_I H_{hf}$, μ_I being the magnetic moment of the excited ^{170}Yb nuclear state. The fluctuation frequencies obtained thereby are reported in Fig.5 and will be discussed below, together with the μSR data.

A first answer to the question about the presence of LRO in $\text{Yb}_2\text{Ti}_2\text{O}_7$ comes from neutron diffraction experiments on a powder sample (performed at the “Laboratoire Léon Brillouin”, Saclay), which reveal there are no magnetic Bragg peaks below 0.24 K. Therefore there is no LRO in $\text{Yb}_2\text{Ti}_2\text{O}_7$ below the temperature of the specific heat peak.

An insight into the dynamics of the moments is further provided by μSR measurements (whose characteristic time is about 10^{-6} s), performed at ISIS (Rutherford Appleton Laboratory, Chilton, England) and at PSI (Villigen, Switzerland) [8]. For all temperatures down to 0.275 K (see Fig.4 a), the time decay of the muon depolarisation has an exponential form:

$$aP_z(t) = a_z \exp(-\lambda_z t) + a_{bg}, \quad (4)$$

where $a_{bg} = 0.065$ is a time independent background contribution arising from muons stopping in the Ag sample holder, and $a_z \simeq 0.17$. These data were recorded in a small longitudinal magnetic field $B_{ext} = 2 \text{ mT}$ in order to suppress the contribution of the nuclear moments to the depolarisation. The relaxation rate λ_z is approximately constant ($\simeq 0.1 \text{ MHz}$) as temperature decreases down to a few Kelvin, then it rises rapidly. An exponential decay for the depolarisation is usually observed when the fluctuation frequency ν of the electronic moments is much larger than the dipolar (and hyperfine) coupling Δ between the muon spin and the electronic spin: $\nu \gg \Delta$ (“extreme narrowing” limit). In this limit and in the paramagnetic phase (i.e.

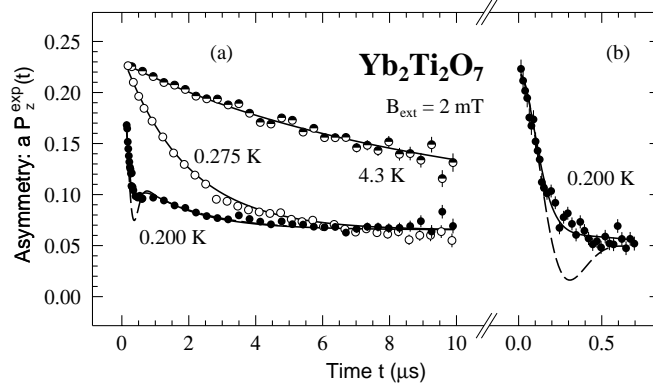


Fig. 4. In $\text{Yb}_2\text{Ti}_2\text{O}_7$: (a) μSR depolarisation spectra, measured at ISIS, on each side of the transition temperature (0.24 K) and (b) detail of the depolarisation at 0.2 K at short times, measured at PSI; the lines are fits as explained in the text.

when the electronic moments are uncorrelated), the following relationship links λ_z and ν :

$$\lambda_z = 2 \frac{\Delta_p^2}{\nu}, \quad (5)$$

where Δ_p is the root mean square deviation of the distribution of dipolar couplings experienced by the muon spin in its interstitial stopping site. The rise of λ_z below about 2 K is thus indicative of a slowing down of the electronic fluctuations as the spin correlations develop. Below the temperature of the specific heat peak (0.24 K), the shape of the muon depolarisation changes drastically (see the 0.2 K data in Fig.4): it is no longer an exponential function of time, but it shows a rapid depolarisation within about 0.2 μs followed by a slow quasi-exponential decay. This shape remains unchanged down to the lowest temperature of the experiment, 0.04 K. The first remarkable thing to notice is that no oscillatory signal is observed, although in this temperature range a hyperfine field is observed in the Mössbauer spectra. This means that no LRO is present, in agreement with the powder neutron diffraction data. The shape of the low temperature depolarisation can actually be accounted for by a dynamic Kubo-Toyabe decay (dashed line in Fig.4), except for a small discrepancy around 0.03 μs : the dip present in the theoretical curve is blurred in the experimental data. A dynamic Kubo-Toyabe lineshape describes the general case of a muon spin coupled to an ensemble of electronic spins with fluctuation frequency ν , and with a root mean square isotropic coupling Δ . Its high frequency limit is an exponential function with a relaxation rate given by expression (5). In order

to reproduce correctly the low temperature depolarisation, a solution consists in introducing a gaussian distribution of Δ values, which could be a means of taking into account the spin correlations [9]. A good fit is thereby obtained (solid line in Fig.4 b), with a rather low fluctuation frequency: $\nu \simeq 10^6 \text{ s}^{-1}$. The mean value of the muon - 4f spin coupling, in units of field, is: $\Delta_{LT}/\gamma_\mu \simeq 5.7 \text{ mT}$, where $\gamma_\mu = 851.6 \text{ Mrd s}^{-1}\text{T}^{-1}$ is the muon gyromagnetic ratio. Thus the presence, below 0.24 K, of a μSR signal consisting of a dynamic Kubo-Toyabe decay and of a hyperfine field in the Mössbauer spectra, means that short range dynamic spin correlations are present down to 0.04 K. The measured μSR fluctuation frequency of 10^6 s^{-1} is accordingly lower than the Mössbauer threshold $\nu_l \simeq 10^8 \text{ s}^{-1}$.

Above the temperature of the specific heat peak, the electronic fluctuation frequencies ν can be deduced from the λ_z values through formula (5) if the high temperature Δ_p value is known and also, in principle, if the spin correlations are weak. Usually, in the paramagnetic phase, fluctuating moments of $1 \mu_B$ (the size of the moments in $\text{Yb}_2\text{Ti}_2\text{O}_7$) correspond to a mean dipolar field of the order of 50 mT. So the mean Δ_{LT} value of 5.7 mT obtained below 0.24 K, where the spin correlations are well developed, is too small and cannot be used at high temperature where correlations are weaker. So in order to extract ν from the λ_z data above 0.24 K, we adjusted Δ_p in expression (5) so that the frequency values match those measured by Mössbauer spectroscopy (see Fig.5). We obtained $\Delta_{HT} \simeq 80 \text{ mT}$, which is the correct order of magnitude. In the paramagnetic phase, Δ_{HT} can be calculated for a known crystal structure by assuming that the muon stops in a given interstitial site (and assuming also a dipolar only interaction with the rare earth spin) [10]. In the present case of an axially symmetric Kramers doublet with g-tensor $\{g_z, g_\perp\}$, Δ_{HT} is given by the expression:

$$\Delta_{HT}^2 = \frac{1}{8\pi g_J^2} [(g_z^2 - g_\perp^2)\Sigma_1 + g_\perp^2 \Sigma_2], \quad (6)$$

where Σ_1 and Σ_2 are lattice sums whose expressions are given in Ref.[10]. There are three possible interstitial sites for the muon in the pyrochlore lattice for which: $\Delta_{HT}/\gamma_\mu \simeq 150 \text{ mT}$. This value is larger by a factor of 2 than that obtained by scaling the μSR data to the Mössbauer data. This is an acceptable agreement, if one keeps in mind that expression (6) is valid for uncorrelated moments only. In fact, at least below 2 K, the specific heat data and the neutron diffraction data on a single crystal (see below) show that spin correlations are present. Therefore, the muon spin is likely to interact with a well defined rare earth moment, of modulus $1.15 \mu_B$ (the low temperature value), within correlated clusters, rather than with a paramagnetic Kramers doublet. With this assumption, the standard calculation

of Δ_{HT} due to randomly oriented moments yields $\Delta_{HT}/\gamma\mu \simeq 80$ mT for the three sites, which is exactly the value derived above.

The overall thermal variation of the Yb spin fluctuation frequency is represented in Fig.5 and constitutes the main result of our study in this compound: the fluctuation frequency undergoes a first order abrupt drop at the temperature of the specific heat anomaly (0.24 K), falling from the 10^4 - 10^5 MHz range to 1 MHz. So the transition involves the time domain and is reminiscent of the liquid-gas transition, which is first order and involves an abrupt drop of the mean collision frequency between atoms as one enters the liquid phase.

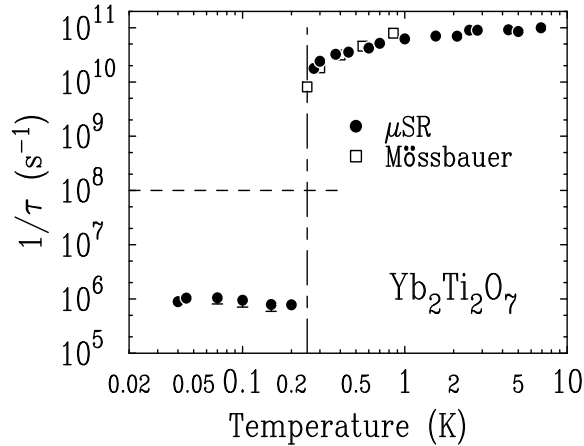


Fig. 5. Thermal variation of the Yb spin fluctuation frequency as measured by μ SR (solid circles) and ^{170}Yb Mössbauer spectroscopy (open squares); the dashed line is the lower limit ν_l of the Mössbauer window for measurement of fluctuation frequencies.

The low temperature phase in $\text{Yb}_2\text{Ti}_2\text{O}_7$ is a “spin-liquid” phase, as predicted by Villain [1] for spins in a lattice of corner sharing tetrahedra, where spin dynamics is present down to the lowest temperature. However, this state is not reached “smoothly” by a continuous decrease of the fluctuation frequency, but by a first order transition in the fluctuation frequency. At this stage, it is not known whether the transition is accompanied by some change in the spatial spin correlations. The answer to this question comes from a neutron diffraction study of a single crystal, to be described next.

The neutron diffraction experiments on a single crystal of $\text{Yb}_2\text{Ti}_2\text{O}_7$ were performed at the Institut Laue Langevin (Grenoble, France), in the temperature range 0.04 K - 30 K. Like the previous neutron diffraction mea-

measurements on a powder sample, no magnetic Bragg peaks were discovered as temperature decreases from 4.2 K to 0.04 K. But mapping of the magnetic elastic scattering in (110) planes reveals the presence of “diffraction rods” along the [111] direction in reciprocal space (see Fig.6). This is indicative of the presence of bidimensional antiferromagnetic spatial correlations, probably within planes perpendicular to [111]. No anomaly is found at 0.24 K: the intensities of the peaks obtained from Q-scans across the rod (see Fig.7 left for the scan along line 1) increase steadily on cooling from about 25 K down to 0.04 K (see Fig.7 right, where the data below 1.4 K are not shown). The width of the peaks in Q-space does not vary with temperature and corresponds to a correlation length $\xi \simeq 4$ nm (about 4 times the parameter of the unit cell, which contains 16 Yb ions). The short range correlations therefore involve a few hundred Yb ions.

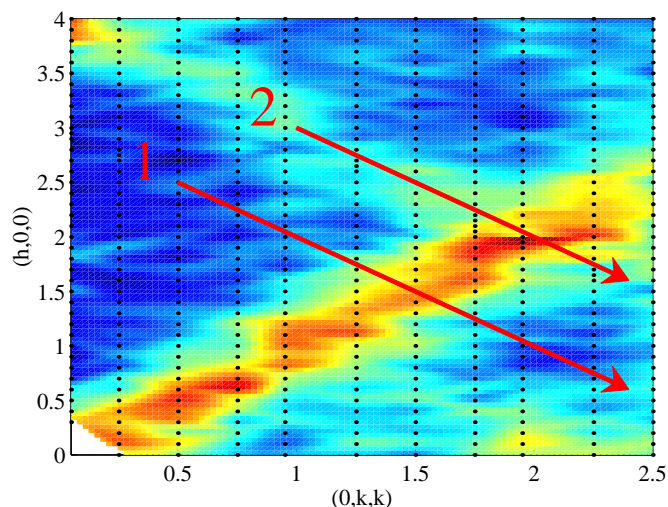


Fig. 6. [color] Map of the magnetic neutron scattering in a single crystal of $\text{Yb}_2\text{Ti}_2\text{O}_7$ in the (110) plane of the reciprocal space at 1.4 K, showing the “diffraction rod” along [111]. The red lines labelled 1 and 2 are the directions along which Q-scans were performed.

The magnetic scattering intensity near $\mathbf{Q}=(1.5,1.5,1.5)$ starts to develop near 25 K, whereas that near $\mathbf{Q}=(1.9,1.9,1.9)$ starts to grow at a lower temperature (about 13 K). Both peaks however reach half their maximum intensity around 2-3 K. This suggests that these spin correlations are driven by the exchange evidenced in the specific heat bump, which has the same energy scale of 2-3 K. The short range bidimensional spin correlations in $\text{Yb}_2\text{Ti}_2\text{O}_7$ thus build up monotonically as temperature decreases; the range

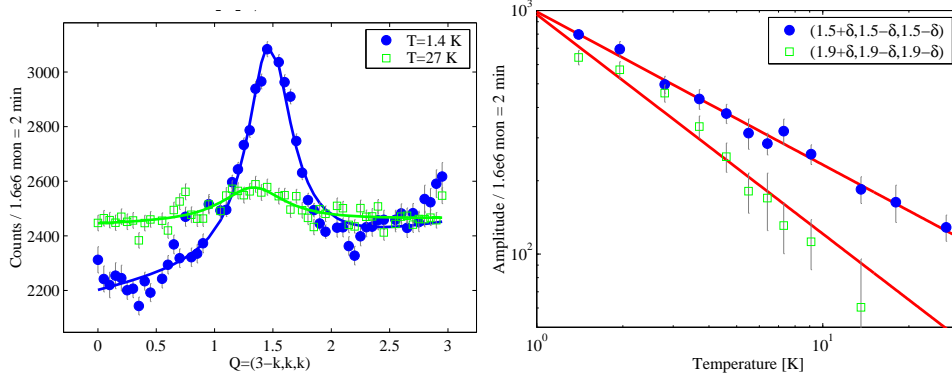


Fig. 7. [color] **Left:** Q -scan across line 1 of the map in Fig.6 at 1.4 and 27 K, and **Right:** thermal variations of the amplitudes of the peaks near $(1.5, 1.5, 1.5)$ across line 1 and near $(1.9, 1.9, 1.9)$ across line 2 of the map in Fig.6.

of these correlations, about 4 nm, is temperature independent and in particular shows no anomaly at 0.24 K. This reinforces the picture sketched above, of a transition involving the frequency domain only.

3. $\text{Gd}_2\text{Sn}_2\text{O}_7$

As shown in the inset of Fig.8 left, the inverse susceptibility in $\text{Gd}_2\text{Sn}_2\text{O}_7$ follows a Curie-Weiss law with a paramagnetic Curie temperature $\theta_p \simeq -10$ K, indicative of an antiferromagnetic exchange interaction. As the Gd^{3+} ion is isotropic, this compound can be therefore expected to be a good realisation of an AF Heisenberg frustrated system, with no Néel order down to $T = 0$. However, both the magnetic susceptibility and the specific heat, shown in Fig.8 right and left respectively, evidence an anomaly at 1 K. The susceptibility $\chi(T)$ presents furthermore a sizeable irreversibility between the FC and ZFC branches below 1 K. The anomaly of the specific heat $C_p(T)$ at 1 K reaches the very large value of $120 \text{ JK}^{-1} \text{ mol. Gd}^{-1}$, whereas the expected jump at T_N for a second order magnetic transition is: $\Delta C_p = \frac{5}{2} R \frac{S(S+1)}{S(S+1)+0.5}$ [11], i.e. $20.4 \text{ JK}^{-1} \text{ mol. Gd}^{-1}$ for Gd^{3+} with $S=7/2$.

This high ΔC_p value is indicative of a first order transition (the specific heat diverges in principle in this case), which will be confirmed by the ^{155}Gd Mössbauer measurements to be described below. Below 1 K, the specific heat varies as T^2 . Classically, the specific heat due to the thermal excitation of magnons in a 3-dimensional Heisenberg AF varies as T^3 , and as T^2 in the bidimensional case. So the observed quadratic variation in $\text{Gd}_2\text{Sn}_2\text{O}_7$ suggests a bidimensional AF structure. The inset of Fig.8 left shows the magnetic entropy variation as temperature increases; at the transition, only

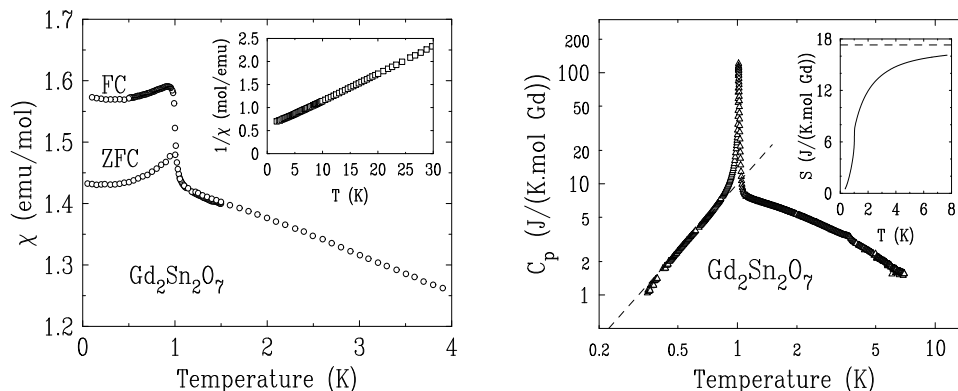


Fig. 8. In $\text{Gd}_2\text{Sn}_2\text{O}_7$: **Left**: magnetic susceptibility measured with 1 mT, with the Field Cooled (FC) and Zero Field Cooled (ZFC) branches; inset: inverse susceptibility below 30 K, and **Right**: thermal variation of the specific heat; the dashed line is a T^2 law; inset: thermal variation of the entropy.

40% of the total entropy $R \ln 8 = 17.3 \text{ JK}^{-1} \text{ mol.Gd}^{-1}$ has been released, and the full paramagnetic degrees of freedom are recovered only at 8-10 K. As in the case of $\text{Yb}_2\text{Ti}_2\text{O}_7$, this is due to the presence of short range order developing well above the transition temperature and it evidences the presence of frustration.

Selected Mössbauer absorption spectra on the isotope ^{155}Gd ($I_g=3/2$, $I_e=5/2$, $E_0=86.5 \text{ keV}$) in $\text{Gd}_2\text{Sn}_2\text{O}_7$ are shown in Fig.9. A clear change in the lineshape is observed between 1.05 and 1.1 K (see Fig.9 left): at 1.1 K and above, the spectrum is a pure quadrupolar hyperfine pattern characteristic of the paramagnetic phase, while at 1.05 K a magnetic hyperfine field has appeared, evidencing short or long range magnetic order. As the temperature is further decreased down to 0.027 K, the hyperfine field increases slightly to reach a saturated value of 30 T. This behaviour is the hallmark of a first order transition, as also inferred from the height of the specific heat peak; in $\text{Gd}_2\text{Sn}_2\text{O}_7$ however, the coexistence region between the two phases could not be detected like in $\text{Yb}_2\text{Ti}_2\text{O}_7$. The fits furthermore show that each Gd^{3+} moment is perpendicular to the [111] local symmetry axis.

The question arises here also as to whether there is LRO below 1 K, or whether the correlated moments fluctuate with a frequency lower than $\nu_l \simeq 3 \times 10^7 \text{ s}^{-1}$, which is the lower limit of the “Mössbauer window” for ^{155}Gd . The answer will be provided by the μSR measurements, but before we turn to their description, we will examine the problem posed by the lowest temperature Mössbauer spectrum.

The spectrum at 0.027 K (see Fig.9 right) indeed deserves particular attention, because the temperature which can be measured from the spectrum

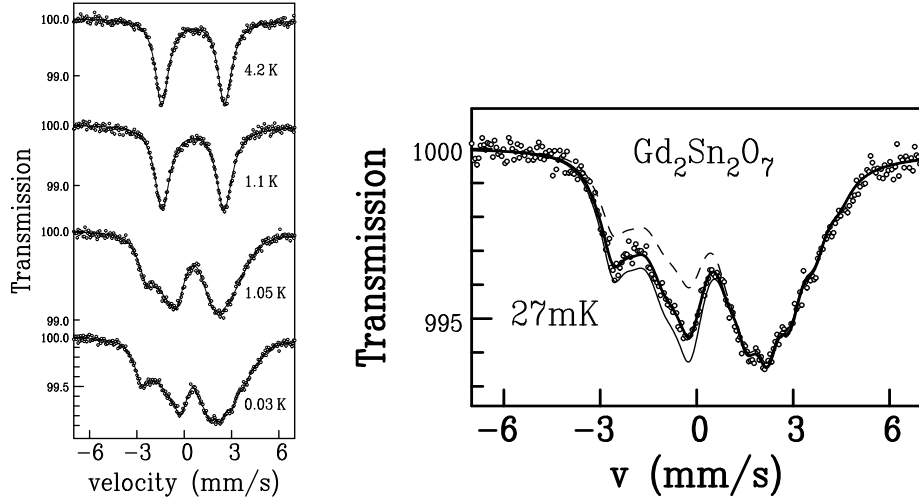


Fig. 9. ^{155}Gd Mössbauer spectra in $\text{Gd}_2\text{Sn}_2\text{O}_7$: **Left**: at selected temperatures between 0.027 K and 4.2 K, and **Right**: at 0.027 K; the lines are theoretical curves for various values of the hyperfine temperature T_{hf} : dashed line, $T_{hf}=0.027\text{ K}$, thick solid line, which fits the data well, $T_{hf}=0.090\text{ K}$, and thin solid line: high temperature limit, $T_{hf} > 0.2\text{ K}$.

($\simeq 0.090\text{ K}$, referred to hereafter as the hyperfine temperature T_{hf}), is much higher than that of the sample (given by the thermometer): $\simeq 0.03\text{ K}$. The possibility of measuring the absolute temperature from the relative line intensities of the Mössbauer spectrum has been since long recognised [12]. The conditions are that the spin I_g of the ground nuclear state is non-zero, and that the hyperfine splittings are of the same order of magnitude as $k_B T$. Then each resonant transition has an intensity which is weighed by the population of the ground hyperfine level it arises from. The temperature of the hyperfine levels (in principle equal to the lattice temperature) can then be obtained directly from the spectrum. This procedure is impossible for ^{170}Yb , which has $I_g=0$, but should work for ^{155}Gd , which has $I_g=3/2$. In $\text{Gd}_2\text{Sn}_2\text{O}_7$, the combined quadrupolar and magnetic hyperfine interactions yield four ground hyperfine levels with energies 0, 0.05, 12.1 and 15.9 mK, i.e. two quasi-degenerate doublets separated by a mean hyperfine splitting $\Delta_{hf} \simeq 14\text{ mK}$. Then the hyperfine temperature can be measured if it is below about 0.15 K. On Fig.9 right are shown, together with the experimental spectrum at 27 mK, the theoretical spectra expected for $T_{hf} = 27\text{ mK}$ (dashed line), for $T_{hf} > 0.2\text{ K}$ (thin solid line) and for $T_{hf} = 90\text{ mK}$ (thick solid line). This last line goes perfectly well through the data points, and it is then clear that the hyperfine levels are “hotter” than the lattice, i.e.

they are out of thermal equilibrium.

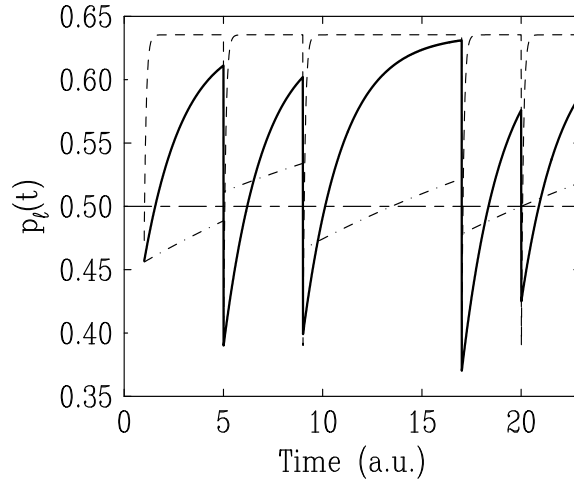


Fig. 10. Temporal evolution of the ground state population $p_\ell(t)$ of a (nuclear) spin 1/2 doublet, as the (hyperfine) field reverses randomly in time, at arbitrarily chosen instants 5, 9, 17 and 20. The ratio of the doublet splitting to $k_B T$ is chosen to be about 2, so that the Boltzmann population of the ground state is 0.63. Dashed line: $T_1 \ll \tau$: thermalisation is effective; dash-dotted line: $T_1 \gg \tau$: thermalisation is impossible, and solid line: $T_1 \sim \tau$.

The interpretation we give for this phenomenon is the following [13]: the hyperfine levels have no time to reach thermal equilibrium, with a time constant T_1 , because the hyperfine field reverses with a time constant τ shorter than or of the same magnitude as T_1 . This is illustrated in Fig.10, which depicts the temporal evolution of the population p_ℓ of the ground state of a fictitious spin 1/2 (modelling the hyperfine levels) as a function of the ratio T_1/τ . The steady state population (i.e. time averaged) $\langle p_\ell \rangle$ is the Boltzmann population p_ℓ^B if hyperfine relaxation occurs very rapidly with respect to τ (dashed line in Fig.10), it is 0.5 (equipopulation) in the reverse case (dash-dotted line in Fig.10), and it should be a function of the ratio $\mu = T_1/\tau$ if the latter is of the order unity (solid line in Fig.10). In order to obtain this function, we devised a model of a spin 1/2 submitted to a magnetic field of constant magnitude, but which undergoes “flips” at random instants of time. The model provided an analytical solution for the steady state population of the ground level:

$$\langle p_\ell \rangle = \frac{1}{2} \left(1 + \frac{1}{1 + 2\mu} \tanh \frac{\Delta}{2k_B T} \right), \quad (7)$$

where Δ is the Zeeman splitting of the spin 1/2 doublet. Assigning to the doublet an effective (in our case hyperfine) temperature (this is always possible for a spin 1/2 system), we obtain: $T_{hf} \simeq T(1 + 2\mu)$ in the range $k_B T > 2\Delta$ which is the temperature range of our experiments. Applying this relation to the case of $\text{Gd}_2\text{Sn}_2\text{O}_7$ yields $\mu \simeq 0.8$.

The fact that the hyperfine populations are out of equilibrium at 0.027 K reveals therefore the presence of two forms of dynamics of the Gd^{3+} electronic spin. The first one consists in spin flips between one (or more) direction(s) which, as the Gd^{3+} moment is proportional to the hyperfine field, correspond to flips of the hyperfine field sensed by the ^{155}Gd nuclear spin. Besides, the nuclear (hyperfine) relaxation, at such low temperature, cannot be due to phonons. The only plausible mechanism is nuclear relaxation driven by coupling to electronic spin-waves [14], which are thus the second form of spin dynamics evidenced at 0.027 K in $\text{Gd}_2\text{Sn}_2\text{O}_7$. The presence of spin-waves at very low temperature is also demonstrated by the μSR experiments, to be described below. The probe in that case is not the nuclear spin of the rare earth atom itself, but the spin of positive muon lying at an interstitial site; the relaxation mechanisms are however similar in both cases.

The μSR experiments were performed in zero magnetic field between 20 mK and 100 K at PSI. Above 1 K, the decay has an exponential form, and the relaxation rate λ_z has a temperature independent value of 2 MHz. Below 1 K, the decay signal changes and presents an oscillating component, indicative of magnetic LRO. The oscillations are clearly visible only at very short times (see Fig.11 left).

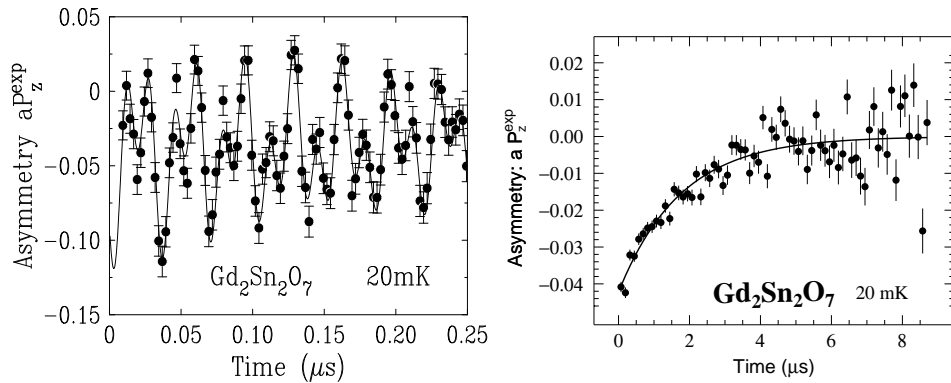


Fig. 11. Time variation of the μSR depolarisation in $\text{Gd}_2\text{Sn}_2\text{O}_7$ at 20 mK, measured at PSI: **Left**: short time part showing the rapidly oscillating components, and **Right**: long time part with a 100 channel binning in order to integrate out the oscillations.

An exponential damping component is also present, which is best visible when the counting channels are grouped into batches of 100 (“binning” of 100 channels), as shown in Fig.11 right where the line is a fit to an exponential function. Usually, in the magnetically ordered phase, the depolarisation in a polycrystalline sample is well described by the following expression (assuming a single stopping site for the muon) [15]:

$$aP_z(t) = \frac{a}{3}[\exp(-\lambda_z t) + 2 \exp(-\lambda_{\perp} t) \cos \omega_{\mu} t]. \quad (8)$$

This is equivalent to a depolarisation function where one third of the impinging muons have their spin parallel to the internal field (first term) and two thirds have their spin precessing in the internal (dipolar) field (second term). In expression (8), a is the amplitude (or asymmetry) of the depolarisation, which in principle does not change when the temperature is lowered through the transition; λ_z is the longitudinal relaxation rate, due to the coupling of the muon spin with the electronic degrees of freedom (in the LRO phase, the spin-waves) [16]; $\omega_{\mu} = \gamma_{\mu} B_i$ is the Larmor frequency of the muon spin in the internal field \mathbf{B}_i , arising from the spontaneous electronic moment, and λ_{\perp} is a damping factor which is generally taken to be due both to a distribution in B_i values and to fluctuations of \mathbf{B}_i . As discussed above, the depolarisation in $\text{Gd}_2\text{Sn}_2\text{O}_7$ below 1 K is described by expression (8) in a first approximation. However, some features are not fully understood at the present time: the asymmetry a below 1 K is half the value above 1 K ($a \simeq 0.2$); there are two oscillating components of equal weights, with dipolar fields of 206 and 441 mT, each with a sizeable phase shift, respectively 24 and 69°. A particular magnetic structure could be at the origin of these peculiarities. We will only mention here that the two dipolar fields are temperature independent between 20 mK and 0.7 K, the highest temperature where the oscillations are clearly visible. The dipolar fields at the muon sites are due to the spontaneous Gd^{3+} moments, and their lack of thermal variation is in line with the Mössbauer spectroscopy finding of an essentially temperature independent moment value, i.e. of a first order transition. Their order of magnitude (200-400 mT) is in agreement with the rough rule stating that a moment of $1 \mu_B$ gives rise to a dipolar field of 50 mT, as the Gd^{3+} saturated moment is $7 \mu_B$.

The thermal variation of the relaxation rate λ_z is shown in Fig.12. Below 1 K, it reflects the muon spin lattice relaxation through the coupling with spin-waves, and it is defined by Eqn.(8); above 1 K, it reflects the fast relaxation due to coupling to the short range correlated, and eventually paramagnetic, Gd^{3+} spins.

The transition at 1 K is marked by a sharp anomaly in $\lambda_z(T)$. The remarkable feature is that λ_z below 1 K shows no thermal dependence, remaining at the constant value 0.6 MHz down to 20 mK. This is anomalous,

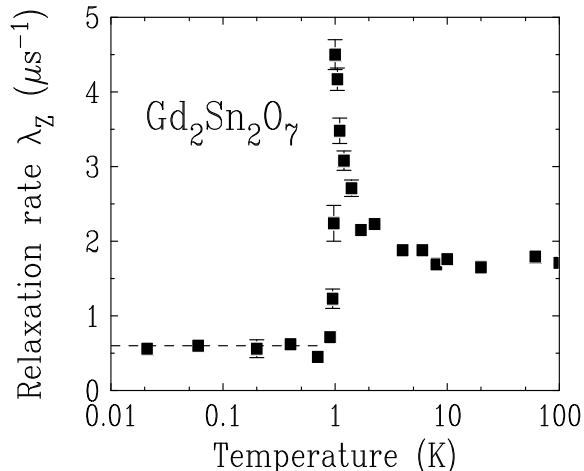


Fig.12. Thermal variation of the muon longitudinal relaxation rate λ_z in $\text{Gd}_2\text{Sn}_2\text{O}_7$. Below 1 K, λ_z is defined by Eqn.(8); above 1 K, it is the relaxation rate of the observed exponential decay (the data for $T \geq 4$ K were obtained with a longitudinal magnetic field of 10 mT). The dashed line at 0.6 MHz underlines the constant relaxation rate below 1 K.

as relaxation of the muon spin by spin-waves should vanish at $T = 0$. For example, it was shown that, for a Heisenberg ferromagnet, λ_z varies as T^2 to a good approximation if one considers two-magnon Raman processes, which are the most likely to occur for relaxation between the quasi-degenerate spin states of the muon [16]. An analogous calculation for a Heisenberg bidimensional AF, which could apply to $\text{Gd}_2\text{Sn}_2\text{O}_7$ as suggested by the specific heat data, yields a T^3 variation. None of these thermal laws matches with experiment. The explanation for the temperature independence of λ_z must probably be looked for in the unusual spin-wave spectrum of $\text{Gd}_2\text{Sn}_2\text{O}_7$, where soft spin-wave modes with a finite density of states at zero energy could exist. A saturation of λ_z below about 2 K has also been observed in another pyrochlore material, $\text{Tb}_2\text{Ti}_2\text{O}_7$ [17]. But this compound shows no phase transition to an LRO phase at low temperature and remains a “correlated paramagnet” down to $T = 0$.

4. Conclusions

Both studied pyrochlore materials, $\text{Yb}_2\text{Ti}_2\text{O}_7$ and $\text{Gd}_2\text{Sn}_2\text{O}_7$, present a low temperature state where spin fluctuations persist as $T \rightarrow 0$.

In $\text{Yb}_2\text{Ti}_2\text{O}_7$, this state seems to be a spin-liquid phase where short range dynamic spin correlations are present. Such a phase is expected for

geometrically frustrated isotropic systems with antiferromagnetic interactions. However, it is not reached by a smooth decrease of the fluctuation frequency as the temperature decreases, but through a first order transition (at 0.24 K) where the spin fluctuation frequency drops from the GHz to the MHz range. Below 0.24 K, this frequency could be measured directly by the μ SR experiments and it remains constant down to 40 mK. No anomaly could be detected at the transition for the spatial spin correlations: they build up from 10-20 K and remain short range, with a correlation length of 4 nm, down to the lowest temperature.

In $\text{Gd}_2\text{Sn}_2\text{O}_7$, the low temperature phase has long range magnetic order and it is reached through a standard first order transition. However, spin dynamics is present down to 30 mK: it was detected indirectly by ^{155}Gd Mössbauer spectroscopy through the finding of nuclear levels which are out of thermal equilibrium. This requires the presence of both electronic spin flips and of nuclear relaxation by coupling to spin waves, with similar characteristic time scales. The presence of spin waves down to 20 mK was also evidenced in the μ SR measurements by the non-vanishing relaxation rate of the μ^+ spin.

These findings illustrate the unconventional dynamics occurring in the frustrated pyrochlores at very low temperature and the diversity of routes leading to a ground state where spin fluctuations persist as $T \rightarrow 0$.

Acknowledgements: We thank A. Forget from SPEC-Saclay for preparing the powder samples and G. Dhahlenne, from LPCES-Orsay, for growing the single crystal $\text{Yb}_2\text{Ti}_2\text{O}_7$ sample. The neutron scattering experiments on this single crystal were performed at the D23 diffractometer at the Institut Laue-Langevin, which is a Collaborating Research Group (CRG) instrument operated by the CEA.

REFERENCES

- [1] J. Villain, *Z. Phys.* **B 33**, 31 (1979)
- [2] for a recent review, see: A. P. Ramirez, in “*Handbook of magnetic materials*”, ed. K. H. J. Buschow (Elsevier) **13**, 423 (2001)
- [3] R. Moessner, T. Chalker, *Phys. Rev.* **B 58**, 12049 (1998)
- [4] H. W. J. Blöte, R. F. Wielinga, W. J. Huiskamp, *Physica* **43**, 549 (1969)
- [5] J. A. Hodges, P. Bonville, A. Forget, M. Rams, K. Królas, G. Dhahlenne, *J. Phys.: Condens. Matter* **13**, 9301 (2001)
- [6] F. Gonzalez-Jimenez, P. Imbert, F. Hartmann-Boutron, *Phys. Rev.* **B 9**, 95 (1974)
- [7] S. Dattagupta, *Hyperfine Interactions* **11**, 77 (1981)

- [8] J. A. Hodges, P. Bonville, A. Forget, A. Yaouanc, P. Dalmas de Réotier, G. André, M. Rams, K. Królas, C. Ritter, P. C. M. Gubbens, C. T. Kaiser, P. J. C. King, C. Baines, *Phys. Rev. Lett.* **88**, 077204 (2002)
- [9] D. R. Noakes, *J. Phys.: Condens. Matter* **11**, 1589 (1999)
- [10] P. Dalmas de Réotier, A. Yaouanc, P. Bonville, *J. Phys.: Condens. Matter* **8**, 5113 (1996)
- [11] H. E. Stanley, “*Introduction to phase transitions and critical phenomena*”, Clarendon Press, Oxford (1971)
- [12] G. K. Shenoy, H. Maletta, *Z. Physik* **269**, 241 (1974)
- [13] E. Bertin, P. Bonville, J.-Ph. Bouchaud, J. A. Hodges, J. P. Sanchez, P. Vulliet, *Eur. Phys. J.* **B 27**, 347 (2002)
- [14] D. Beeman, P. Pincus, *Phys. Rev.* **166**, 359 (1968)
- [15] A. Schenck, “*Muon spin rotation spectroscopy*”, Adam Hilger Ltd (Bristol, 1985)
- [16] P. Dalmas de Réotier, A. Yaouanc, *Phys. Rev.* **B 52**, 9155 (1995)
- [17] J. S. Gardner, S. R. Dunsiger, B. D. Gaulin, M. J. P. Gingras, J. E. Greedan, R. F. Kiefl, M. D. Lumsden, W. A. MacFarlane, N. P. Raju, J. E. Sonier, I. Swainson, Z. Tun, *Phys. Rev. Lett.* **82**, 1012 (1999)